stichting
mathematisch
centrum

MC

AFDELING TOEGEPASTE WISKUNDE
(DEPARTMENT OF APPLIED MATHEMATICS)

TW 221/82 MAART

J. GRASMAN, H. NIJMEIJER & E.J.M. VELING

SINGULAR PERTURBATIONS AND A MAPPING ON AN INTERVAL FOR THE FORCED VAN DER POL RELAXATION OSCILLATOR

Preprint

kruislaan 413 1098 SJ amsterdam

Printed at the Mathematical Centre, 413 Kruislaan, Amsterdam.

The Mathematical Centre, founded the 11-th of February 1946, is a non-profit institution aiming at the promotion of pure mathematics and its applications. It is sponsored by the Netherlands Government through the Netherlands Organization for the Advancement of Pure Research (Z.W.O.).

1980 Mathematics subject classification: 34C15, 34D15, 34E05, 58F12, 58F13, 58F15, 58F21, 58F22

Singular perturbations and a mapping on an interval for the forced Van der Pol relaxation oscillator *)

by

J. Grasman, H. Nijmeijer & E.J.M. Veling

ABSTRACT

This paper deals with the Van der Pol relaxation oscillator with a large sinusoidal forcing term. By using singular perturbation techniques asymptotic solutions of such a system are constructed. These asymptotic approximations are locally valid and may take the form of a two time scale expansion in one region and a boundary layer type of solution in a next region. Integration constants are determined by averaging and matching conditions. From these local solutions a difference equation is constructed. There is an equivalence between solutions of the difference equation being an iterated mapping on a compact interval and solutions of the system itself. This equivalence makes it possible to analyze subharmonics and chaotic type of solutions to the full extent. As a result of this we find domains in the parameter space, where regular subharmonics exist. These domains overlap so that for some parameter values different subharmonics coexist. For the same values chaotic type of solutions are found as well. They are described by using concepts of symbolic dynamics.

KEY WORDS & PHRASES: *Van der Pol equation, forced relaxation oscillation, asymptotic expansion, mapping on an interval, strange attractor*

---

*) This report will be submitted for publication elsewhere.

1. INTRODUCTION

Recent studies of difference equations [14,18,25] have revealed unexpected phenomena which in literature are characterized by the term "chaotic". Some of these equations are meant to model biological phenomena such as the from year to year changing densities of biological populations. It has been found that differential equation models with state variables depending continuously on time may too exhibit chaotic behavior. The Lorenz equations, a "simple" model for the onset of turbulence in the context of meteorological problems, is a well-known example of such a system, see [17,21]. It is understood, that this system contains a so-called strange attractor.

In electronic circuits it has been observed that periodically forced nonlinear oscillators may behave chaotically in certain parameter ranges [4,16]. In this paper we carry out an asymptotic analysis of such a system, the forced Van der Pol oscillator,

$$\frac{d^2x}{dt^2} + \nu(x^2-1)\frac{dx}{dt} + x = (\alpha\nu+\beta)k \cos kt, \qquad 0 < \alpha < 2/3 \tag{1.1}$$

for large values of ν. Eventually, we will construct a difference equation that contains all necessary quantitative and qualitative information for describing the possible solutions of this system. Besides the well-known stable solutions of period $T = 2\pi(2n-1)$, also irregular types of solutions are analyzed. Existence of such solutions was expected by LITTLEWOOD [15] and made plausible by LEVINSON [13] in a study of a related piece-wise linear equation. The horse shoe mapping created by SMALE [23,24] turned out to be an important tool in establishing the existence of these irregular solutions. LEVI [11,12] used this concept and symbolic dynamics (see also GUCKENHEIMER [10]) in his study of a modified version of (1.1) which comes close to the piece-wise linear variant of Levinson. Our results agree qualitatively with those of Levi. Furthermore, (1.1) has been solved numerically by FLAHERTY & HOPPENSTEADT [3]. A comparison shows that there is also a good agreement between the outcome of their work and that of our asymptotic investigation.

In Section 2 we give a qualitative description of the solutions of

(1.1). Most of it is based on the work of Levi. Matched local asymptotic solutions of (1.1) are constructed in section 3. We only present those results that are needed for deriving the mapping on an interval. For more details of this aspect of our analysis we refer to [6,7]. Furthermore, an analogous analysis has been made in [8,9] and [5], where the cases $\alpha = 0$ and $\alpha = 2/3$ have been worked out. The solution of the case we have under consideration now ($0<\alpha<2/3$) exhibits phenomena that are met in these extreme cases separately. In section 4 we give the interval mapping in the form of a set of asymptotic relations. It is noticed that the domain of the interval mapping is related with the order of a parabolic cylinder function being an asymptotic approximation of the solution in a critical region of the state space where many diverging trajectories meet each other at short distance. This choice of the interval comes up in a natural way and shows that the asymptotic approach discloses characteristics of the system, that would have remained unnoticed in a different type of analysis of the problem.

From the asymptotic interval mapping the qualitative properties of (1.1) are found and a numerical approximation is made. In section 4.2 we construct the regions in the parameter space, where regular subharmonics exist. Moreover, in section 4.6, we trace a stable irregular periodic solution by using this numerical approximation of the interval mapping.

2. THE ANNULUS MAPPING AND SYMBOLIC DYNAMICS

2.1. Properties of the Poincaré mapping

Following LEVI [11] we consider (1.1) in the form of a system of two first order differential equations

$$\dot{x} = \nu(y-1/3x^3+x) \tag{2.1a}$$

$$\dot{y} = -x/\nu+b\cos kt, \qquad b = (\alpha+\beta\nu^{-1})k, \tag{2.1b}$$

and introduce the Poincaré mapping D:

(2.2) $\quad D(x(0),y(0)) = (x(2\pi),y(2\pi)).$

It can be shown that a properly chosen annulus A in the x,y-plane is mapped into an annulus A' under D^m for m sufficiently large with A' having a thickness $O(\exp(-c\nu^2))$ near the branches of $y = 1/3x^3-x$ and of order $O(\nu^{-\frac{1}{2}})$ at the horizontal parts where it jumps from one branch to the other, see fig. 1. Within the annulus A' one may cut out a small part R such that for all $s = (x,y) \in A, D^j s \in R$ for certain $j \in \mathbb{N}$. Note that there is even an infinite sequence j_k, $k = 1,2,\ldots$ with $D^{j_k}s \in R$. Therefore it is sufficient to study the mapping $\hat{P}:R \to R$, where $\hat{P}s = D^j s$ with j being the first integer for which $D^j s \in R$. By taking $\hat{P}(s) = s$ for $s \in R$ we obtain a continuous mapping $\hat{P}$ on R. Identification of the upper and lower sides of R makes R an annulus. Note that no points in R correspond with each other under $\hat{P}$. Thus, the study of the Poincaré mapping D is reduced to the analysis of the annulus mapping $\hat{P}:\bar{R} \to \bar{R}$. Because of the symmetry with respect to the origin there is a same area R' in the opposite quadrant of the x,y-plane. Clearly, it is sufficient to study the mapping $P:\bar{R} \to \bar{R}'$ as $\hat{P} = P \circ P$.

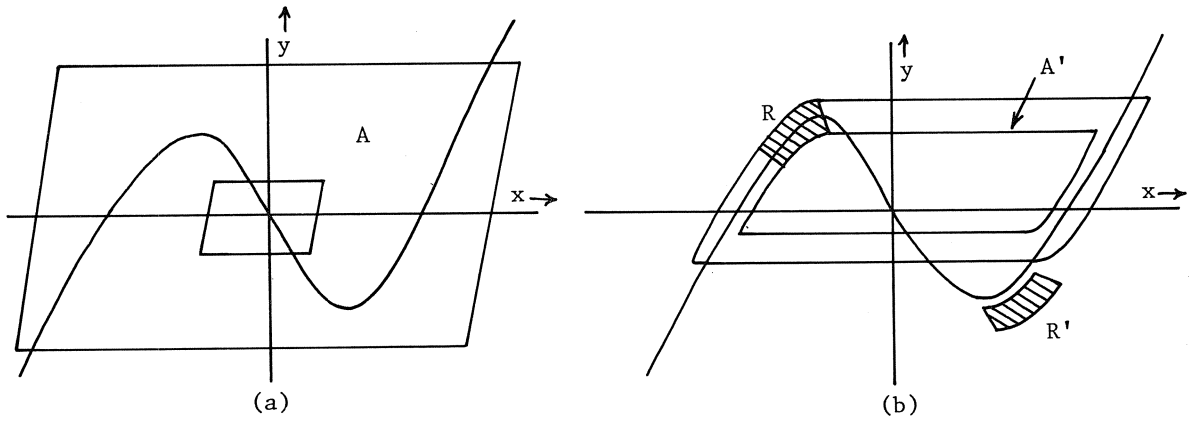

Fig. 1. Contraction of an annulus by repeated mappings D.

2.2. A circle mapping

In a first approach we ignore the thickness of R and interprete P as a circle mapping from S^1 to S^1. Graphically P behaves qualitatively as

follows (see fig. 2). A small arc Δ of order $O(\nu^{-1})$ of S^1 is strectched by P to, say, 1.5 times the length of S^1, while the remaining part $S^1 \setminus \Delta$ is deformed simply by closing the image of Δ. As we will find out, an increase of the forcing b means a clockwise rotation of the image $P(\Delta)$. This immediately leads to the presentation in fig. 3, where for two different values of b we have given the graph of P. The two cases $\tilde{A}$ and $\tilde{B}$ correspond to mappings P with quite different properties. LEVI [11] makes these differences visible in the associated graphs of the annulus mapping P with R being essentially an annulus and not a circle.

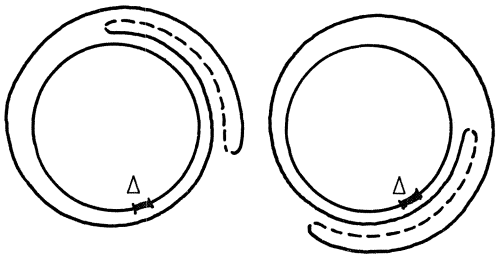

Fig. 2. Circle mapping

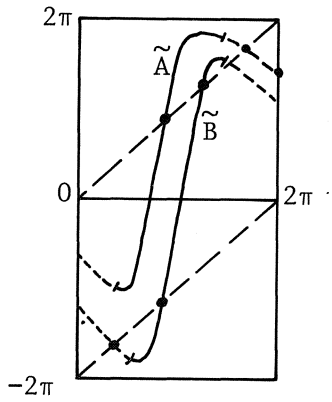

Fig. 3. Graphs of two cases

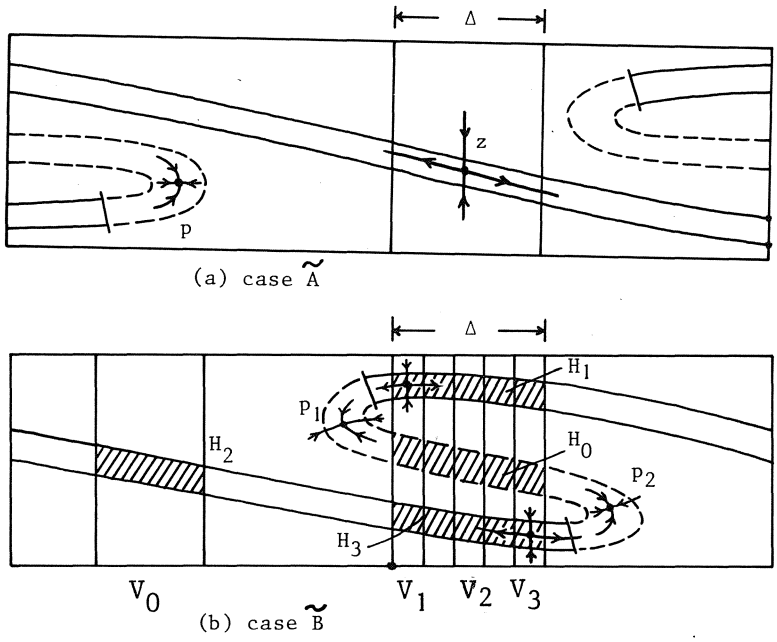

Fig. 4. The annulus mapping

2.3. The annulus mapping

In fig. 4a we depicted the simple configuration of one stable fixed point p and an unstable saddle point z for the mapping P. By rotation we arrive at the more complicated configuration of fig. 4b: it has two stable fixed points p_1, p_2 and two unstable saddle point type of fixed points z_1 and z_2. There is still another set of points C, which cannot decide to which basin of attractors they belong. C is a Cantor set of measure zero, which is invariant under P. In fact C contains a nontrivial "attractor" of the type known as the horseshoe, see SMALE [23,24]. Symbolic dynamics (see e.g. [22]) gives a description of P restricted to C, see MOSER [19]. We set

$$\Delta \cap P(\Delta) = H_1, H_2, H_3, \tag{2.3a}$$

see fig. 4b, and define V_0, V_1 and V_3 by

$$P(V_i) = H_i, \qquad i = 0,1,3. \tag{2.3b}$$

Furthermore, let $H_2 = V_0 \cap P(\Delta)$, then V_2 is defined by

$$P(V_2) = H_2. \tag{2.3c}$$

We now introduce the transition matrix M by

$$M_{ij} = 0, \quad \text{if } V_i \cap H_j \neq \emptyset$$

and

$$M_{ij} = 1 \quad \text{else,}$$

so

$$M = \begin{pmatrix} 0 & 1 & 1 & 1 \\ 0 & 1 & 1 & 1 \\ 1 & 0 & 0 & 0 \\ 0 & 1 & 1 & 1 \end{pmatrix} . \tag{2.4}$$

2.4. The use of symbolic dynamics

The basic idea of symbolic dynamics is to introduce a space Σ of all possible biinfinite strings of a given set of symbols. Referring to the indices of V_i and H_i of section 2.3 we take the symbols 0,1,2 and 3:

$$\Sigma = \{0,1,2,3\}^{\mathbb{Z}}.$$

Thus, an element $\underline{a} = (\ldots,a_{-1},a_0,a_1,\ldots) \in \Sigma$ may read

$$\ldots 01121322110\ldots \quad .$$

By posing restrictions upon the type of symbol that follows a given symbol one introduces a subspace of Σ:

$$\Sigma_M = \{\underline{a} \in \Sigma \,|\, M_{a_i a_{i+1}} = 1\}.$$

Let M be given by (2.4). The mapping $P:C \to C$ is topologically conjugate with the shift $\sigma: \Sigma_M \to \Sigma_M$, where σ satisfies

$$[\sigma(\underline{a})]_i = a_{i+1}, \quad i \in \mathbb{Z}.$$

Thus, there is a one to one corresponding θ between C and Σ_M:

$$\begin{array}{ccc} C & \xrightarrow{P} & C \\ {\scriptstyle\theta}\downarrow & & \downarrow{\scriptstyle\theta} \\ \Sigma_M & \xrightarrow{\sigma} & \Sigma_M \end{array}$$

2.5. Some remarks about the annulus mapping

Returning to the annulus (or circle) mapping we observe the following

dependence of this mapping upon b. There is a subdivision of the b-interval (0,2/3) into subintervals $\tilde{A}_k$ and $\tilde{B}_k$ separated by small intervals $\tilde{g}_k$, such that for $b \in \tilde{A}_k$ P acts as given in fig. 4a (or fig. 2a), while for $b \in \tilde{B}_k$ the behavior can be understood from fig. 4b (or fig. 2b). In summary we conclude that for $b \in \tilde{A}_k$ there is only one stable solution and except for one saddle point all solutions tend to this stable one. For $\beta \in \tilde{B}_k$ two stable solutions exist. Except for a Cantor set of measure zero all solutions tend to one of the attractors.

As b crosses a separation interval $\tilde{g}_k$ there is a sequence of bifurcations and the remarkable phenomenon occurs that for uncountably many $b \in \tilde{g}_k$ there exist infinitely many stable fixed points of P or of its iterates (see e.g. NEWHOUSE & PALIS [20]). In trying to understand this complicated bifurcation pattern we need more information about the mapping P. Intuitively, it is felt that these bifurcations are related with the disappearance of intersections $V_i \cap H_j$, see fig. 4b, and that therefore certain finite sequences in Σ_M are forbidden.

It is obvious that an exact description of the mapping P on the interval as sketched in fig. 3 is the first step in the full understanding of the bifurcation pattern. It is our goal to give a complete description of this mapping and its dependence upon the parameters. In the following sections we will construct matched local asymptotic solutions of (1.1), which eventually lead to a mapping on an interval with the same properties as P.

Finally, it is noted that the study of interval mappings has become a field of growing importance in the analysis of dynamical systems, see e.g. [20]. Various bifurcation problems have been solved by using the concept of mapping on an interval, but there still remain many questions about the exact description of families of interval mappings. In particular we mention the chaotic behavior of mappings within certain parameter ranges.

3. MATCHED LOCAL ASYMPTOTIC SOLUTIONS

3.1. Outline of the method

A solution of (1.1) has a behavior that is characteristic for singular perturbation problems. Locally the solution exhibits a boundary layer type

of action like one meets in problems of fluid mechanics. On the other hand it passes a large time interval, where a two time scales expansion can be applied. Finally, we distinguish a sequence of points, determined by the intersections with the lines $x = \pm 1$, where the local behavior of the solutions is analyzed by a stretching procedure in both the dependent and independent variable. For a complete picture of the different regions which are successively crossed by the solution we refer to fig. 5 . The method of matched asymptotic expansions (see e.g. [1]) yields formal local asymptotic solutions in which the integration constants are determined by averaging conditions and by matching pairs of local solutions of adjacent regions. These computations have been carried out in [6,7]. In the next sections we summarize the results. It is emphasized that this approach is formal and that, for the type of problem we are dealing with, there is no proof of correctness that justifies this approach. However, the present method results in a clear qualitative picture of the solution and, in addition, provides us with quantitative information about the existence of subharmonic and other solutions. Comparing this outcome with analytical and numerical results for the same or related problems [3,11], we observe an excellent agreement. Furthermore, matching methods require a high degree of internal consistency. That is: two neighboring local solutions match, if they exhibit the same behavior in a relatively broad domain of overlap. This type of consistency we also meet in the final result: we analyse here the case $0<\alpha<2/3$ and derive conditions for β in order to have a subharmonic of order n. In the limit $\alpha \to 0$ and $\alpha \to 2/3$ these conditions need to match the ones obtained from studying the special cases $\alpha = 0$ and $\alpha = 2/3$, see [5,8]. As we will see this turns out to be correct indeed.

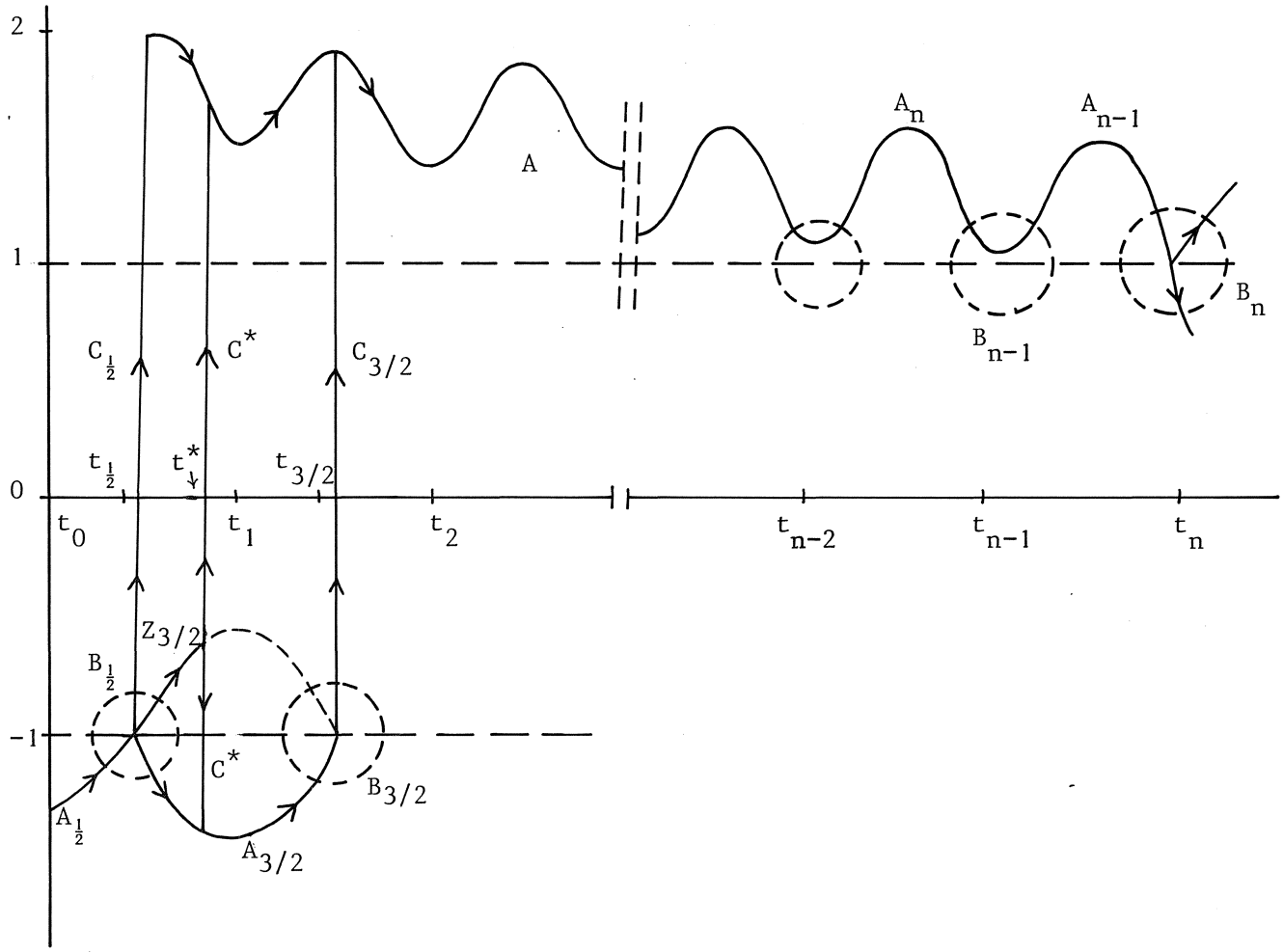

Fig. 5. Regions for local asymptotic solutions

3.2. A two time scales expansion

For the region A of fig. 5 we assume that the solution can be expanded as

(3.1a) $$x = x_0(t,\tau) + \nu^{-1}x_1(t,\tau) + \nu^{-2}x_2(t,\tau)+\ldots,$$

(3.1b) $$\tau = (t-t^*)/\nu, \quad t_{1/2} \le t^* \le t_{3/2}$$

with

(3.1c) $t_r = (-\pi/2+2\pi r)/k,$

(3.1d) $x_0 = 2\cos[\frac{1}{3}\arccos\{\frac{3}{2}\alpha\sin kt + \frac{3}{2}C_0(\tau)\}],$

(3.1e) $(x_0^2-1)x_1 = -\frac{\partial x_0}{\partial t} - \int_{t^*}^{t} x_0(\bar{t},\tau)d\bar{t} - (t-t^*)\frac{\partial C_0}{\partial \tau} + \beta\sin kt + C_1(\tau),$

(3.1fg) $\frac{\partial C_0}{\partial \tau} = \frac{-k}{2\pi}\int_{\tau\nu}^{\tau\nu+2\pi/k} x_0(t,\tau)dt, \quad C_0(0) = 2/3-\alpha,$

(3.1h) $C_1(\tau) = q(\tau)\{C_{10}-\beta p(\tau)\}, \qquad C_1(0) = C_{10},$

(3.1i) $q(\tau) = \exp\{\frac{-k}{2\pi}\int_0^{\tau}\int_{\bar{\tau}\nu}^{\bar{\tau}\nu+2\pi/k}\frac{1}{x_0^2-1}\,dt\,d\bar{\tau}\}$

(3.1j) $p(\tau) = \frac{k}{2\pi}\int_0^{\tau}\exp\{\frac{k}{2\pi}\int_0^{\bar{\tau}}\int_{\hat{\tau}\nu}^{\hat{\tau}\nu+2\pi/k}\frac{1}{x_0^2-1}\,dt\,d\hat{\tau}\}\int_{\bar{\tau}\nu}^{\bar{\tau}\nu+2\pi/k}\frac{\sin kt}{x_0^2-1}\,dt\,d\bar{\tau}.$

The solution will leave the region A at a time t_m, see (3.1c), when it approaches the line $x = 1$, which is the case if C_0 reaches the value $\alpha - 2/3$. From (3.1fg) it follows that in the slow time scale this will be for

(3.2) $T = \frac{-2\pi}{k}\int_{2/3-\alpha}^{-2/3+\alpha}\{\int_0^{2\pi/k} x_0(t;C_0)dt\}^{-1}\,dC_0.$

3.3. Other local asymptotic solutions

For a region A_m, which is entered by the solution in a neighborhood of $(x,t) = (1,t_{m-1})$ and left near $(x,t) = (1,t_m)$, the local asymptotic solution reads

(3.3a) $x = x_0^{(m)}(t) + \nu^{-1}x_1^{(m)}(t) + \nu^{-2}x_2^{(m)}(t)+\ldots,$

(3.3b) $x_0^{(m)} = 2\cos\{\frac{1}{3}\arccos(\frac{3}{2}\alpha\sin kt + \frac{3}{2}C_0^{(m)}) + \frac{2}{3}\pi j\}$

(3.3cd) $C_0^{(m)} = \alpha - 2/3, \quad j = 0,$

$$(3.3e)\qquad \{(x_0^{(m)})^2-1\}x_1^{(m)} = \frac{-dx_0^{(m)}}{dt} - \int_{t_{m-1}}^{t} x_0^{(m)}(\bar{t})d\bar{t} + \beta \sin kt + C_1^{(m)}.$$

For the $\nu^{-\frac{1}{2}}$-neighbourhood of $(x,t) = (1,t_m)$, that is region B_m, we have

$$(3.4ab)\qquad x = 1 + \nu^{-\frac{1}{2}}V_0(m)(\xi) + \nu^{-1}V_1^{(m)}(\xi)+\ldots, \quad \xi = (t-t_m)\nu^{\frac{1}{2}},$$

$$(3.4c)\qquad V_0^{(m)} = -a\, D'_{K_m/a^2}(-a\xi)/D_{K_m/a^2}(-a\xi), \qquad a = \sqrt[4]{2\alpha k^2},$$

$$(3.4d)\qquad K_m = -a^2/2 + (-C_1^{(m)} + \beta + 2\pi I) = -a^2/2 + (-C_1^{(m+1)}+\beta)$$

$$(3.4e)\qquad I = \frac{1}{2\pi}\int_{t_{m-1}}^{t_m} x_0^{(m)}(t)dt, \quad K_{m+1} = K_m + 2\pi I,$$

where in (3.4c) $D_\mu(z)$ denotes the parabolic cylinder function of order μ. For $\mu \le 0$ $D_\mu(z)$ has no zero's. Let us assume, therefore, that $K_m < 0$. It is found that for $t = t_m$ with $x(t_m) = 1 + O(1)$ and with $\{x(t_m)-1\}^{-1}\nu^{-\frac{1}{2}} \to 0$ as $\nu \to \infty$ the following matching relation holds

$$(3.4f)\qquad C_1^{(m)} = C_1(T) - 2\pi(m-3/2)I + kIT\nu.$$

3.4. A boundary layer type of local asymptotic solution

If for the region $B_{1/2}$ the constant $K_{1/2}$ is positive and bounded away from zero (independent of ν), the solution will enter the boundary layer region $C_{1/2}$ with local variable

$$(3.5a)\qquad \eta = (t-t_{1/2}-\xi_0\nu^{-\frac{1}{2}})\nu,$$

where ξ_0 is the value of ξ for which the denominator of (3.4c) vanishes. For this region we introduce the boundary layer expansion

$$(3.5b)\qquad x = W_0(\eta) + \nu^{-1}W_1(\eta) + \nu^{-2}W_2(\eta)+\ldots,$$

where W_0 and W_1 satisfy the equations

(3.5c) $$(1-W_0)^{-1} + 1/3\log\{(W_0+2)(1-W_0)^{-1}\} = -\eta + H_0,$$

(3.5d) $$W_1' + (W_0^2-1)W_1 = 1/4a^4\xi_0^2 - 1/2a^2 - K_{1/2}.$$

Notice that $W_0 \to 2$ as $\eta \to \infty$. Apparently, the boundary layer solution matches the solution for region A given by (3.1) provided that

(3.5e) $$C_{10} = K_{1/2} + 1/2a^2 - \beta.$$

If $K_{1/2} < 0$ and $K_{3/2} > 0$, the solution first passes the region $A_{3/2}$, where it satisfies (3.3) with $j = 1$ and $C_0^{(3/2)} = -\alpha + 2/3$. Next, in region $B_{3/2}$ it satisfies (3.4) and, finally, it enters the boundary layer region $C_{3/2}$, where (3.5) holds with $t_{1/2}$ replaced by $t_{3/2}$. It matches the solution of region A if

(3.5f) $$C_{10} = K_{3/2} + 1/2a^2 - \beta.$$

3.5. Balancing on an unstable branch: dips and slidings

In this section we consider the case where

(3.6a) $$K_{1/2} = \sigma \exp(-d\nu)$$

with $\sigma = \pm 1$. This choice of $K_{1/2}$ will produce a local behavior near the line $x = -1$, which we indicate by dips and slidings of the solution. In the $B_{1/2}$-region the solution takes the form

(3.6b) $$x = \hat{x}(t_{1/2}+\xi\nu^{-\frac{1}{2}};\nu) + v(\xi)\nu^{-\frac{1}{2}}e^{-d\nu},$$

where $\hat{x}$ is the regular expansion (3.3) valid in a O(1) neighborhood of $t = t_{1/2}$. For $t \le t_{1/2}$ we have that $m = 1/2$ and $j = 1$, while for $t \ge t_{1/2}$ we must take $m = 3/2$ and $j = 2$. For the integration constant in the leading term (3.3b) we have the same value

(3.6c) $$C_0^{(1/2)} = C_0^{(3/2)} = -\alpha + 2/3.$$

For $v(\xi)$ in (3.6b) we obtain

$$(3.6d) \qquad v = -\sigma\, a \exp(a^2\xi^2/4) D_{-1}(-a\xi).$$

As the solution leaves the $B_{1/2}$-region the perturbation term v grows rapidly. This process continues in the $Z_{3/2}$-region where

$$(3.7a) \qquad x \approx \hat{x}(t;\nu) + V(t;\nu),$$

$$(3.7b) \qquad V = \sigma \exp\{-\nu(A(t)+d)\}[-a\nu^{-\frac{1}{2}}\sqrt{2\pi} - a^2 \int_{t_{1/2}}^{t} \exp\{\nu A(\bar{t})\} d\bar{t}],$$

$$(3.7c) \qquad A(t) = \int_{t_{1/2}}^{t} \{\hat{x}^2(\bar{t};0)-1\} d\bar{t}.$$

This asymptotic solution brakes down as t approaches t^* satisfying

$$(3.8) \qquad A(t^*) = -d.$$

Assuming that $t^* < t_{3/2}$ we have to introduce another boundary layer type of solution for the region C^*

$$(3.9ab) \qquad x = W_0(\eta) + \nu^{-1} W_1(\eta) + \ldots, \qquad \eta = (t-t^*)\nu$$

with W_0 satisfying

$$(3.9c) \qquad \frac{\ell n|W_0-z_*|}{z_*^2-1} + \frac{\ln|W_0-a_*|}{a_*^2-1} + \frac{\ln|W_0-x_*|}{x_*^2-1} = -\eta + \frac{\ln|-\sigma a\sqrt{2\pi/\nu}/2|}{z_*^2-1},$$

in which $z_* = \hat{x}(t^*;0)$ and a_* and x_* are the two other roots of the algebraic equation

$$(3.9d) \qquad 1/3 W_0^{\,3} - W_0 = 1/3 z_*^{\,3} - z_*$$

with $a_* < -1$ and $x_* > 1$. For W_1 we have

$$(3.9e) \qquad W_1' + (W_0^{\,2}-1)W_1 = \alpha\eta k \cos kt^* - \int_{t_{1/2}}^{t^*} \hat{x}(t;0)dt + \beta \sin kt^* - \beta + \tfrac{1}{2}a^2.$$

Taking $\sigma = 1$ we find that $W_0 \to x_*$ as $\eta \to \infty$ and matches the solution of region A, see (3.1), if

$$(3.10a) \qquad C_{10} = -\beta + \tfrac{1}{2}a^2 - \int_{t_{1/2}}^{t^*} \hat{x}(t;0)dt.$$

For $\sigma = -1$ W_0 tends to the other stable root $a^* < -1$ and matches the asymptotic solution for region $A_{3/2}$ given by $x = \hat{a}(t;\nu)$ satisfying (3.3) with $j = 1$, $C_{a_0}^{(3/2)} = -\alpha + 3/2$ and

$$(3.10b) \qquad C_{a_1}^{(3/2} = C_1^{(3/2)} + \int_{t_{1/2}}^{t^*} \hat{x}(t;0)dt.$$

In the $B_{3/2}$-region (3.4) is valid with

$$(3.11) \qquad K_{3/2} = -\int_{t_{1/2}}^{t^*} \hat{x}(t;0)dt - \int_{t^*}^{t_{3/2}} \hat{a}(t;0)dt.$$

After crossing the unstable interval $|x| < 1$, it arrives at the region A, where it matches (3.1) because of (3.5f).

In [7] the case where d is sufficiently large (including $\sigma = 0$) has been studied in detail. Then $t^* = t_{3/2}$ and a special type of local solution is valid in the $B_{3/2}$-region. We no not present this result here as it does not affect the matching relations given above.

4. MAPPING ON AN INTERVAL

4.1. The formula for the interval mapping

Using the matched local asymptotic solutions of the foregoing sections, we will relate the value K_n of the B_n-region (n a positive integer) with the value of $K_{1/2}$. We restrict $K_{1/2}$ to a compact interval X of length $2\pi I$ and take for n the first positive integer for which K_n returns in this interval. In this way we constructed a mapping P of X into itself. From (3.1h), (3.4d), (3.4f) and (3.5ef) it follows that for $K \in X$, excluding any exponentially small (with respect to ν) neighborhood of $K = 0 \mod(2\pi I)$

(4.1a) $PK = -qK + R(n(K))$

with

(4.1b) $R = (1+q+pq)\beta - \frac{1}{2}a^2(1+q) + 2\pi(n-\frac{1}{2})I - kI\mathcal{T}\nu,$

where $p = p(\mathcal{T})$ and $q = q(\mathcal{T})$ are given by (3.1ij). It is remarked that n may jump to $n \pm 1$ as K varies over X in order to keep PK within X. Furthermore, near $K = 0$ the relations (3.1b) and (3.10a) hold, so we have

(4.1c) $PK = C^+(t^*) + R(n(K))$

with

(4.1d) $$C^+(t^*) = q\int_{t_{1/2}}^{t^*} \hat{x}(t;0)dt - Ik(t^*-t_{1/2})$$

and K and t^* such that

(4.1e) $K = \exp(-d\nu)$

(4.1f) $$\int_{t_{1/2}}^{t^*} \{\hat{x}^2(t;0)-1\}dt = -d.$$

On the other hand for

(4.1g) $K = -\exp(-d\nu)$

we have

(4.1h) $PK = C^-(t^*) + R(n(K))$

(4.1i) $$C^-(t^*) = q\{\int_{t_{1/2}}^{t^*} \hat{x}(t;0)dt + \int_{t^*}^{t_{3/2}} \hat{a}(t;0)dt\}-2\pi I$$

with t^* satisfying (4.1f). It is observed that for $d \to \infty$ (4.1c) matches (4.1h) as then $t^* \to t_{3/2}$, s-e (4.1d) and (4.1i). Moreover, (4.1c) and (4.1h)

match (4.1a) as $d \to 0$.

4.2. A discontinuous approximation of the mapping

In a first approach of describing the mapping (4.1) we let formally $\nu \to \infty$ and consider PK for the interval $(0,2\pi I)$, see fig. 6. The mapping has a fixed point that corresponds with a symmetric solution of period $2\pi(2n-1)/k$ for

$$\underline{\beta}_n(\alpha;\nu) < \beta < \bar{\beta}_n(\alpha;\nu) \tag{4.2a}$$

with

$$\underline{\beta}_n = \{\tfrac{1}{2}a^2(1+q)-H_n(\alpha,\nu)\}/S, \tag{4.2b}$$

$$\bar{\beta}_n = \{(\tfrac{1}{2}a^2+2\pi I)(1+q)-H_n(\alpha,\nu)\}/S, \tag{4.2c}$$

$$H_n = \{2\pi(n-\tfrac{1}{2})-kT\nu\}I \tag{4.2d}$$

$$S = 1+q+pq. \tag{4.2e}$$

Since $\underline{\beta}_n < \bar{\beta}_{n+1} < \underline{\beta}_{n-1} < \bar{\beta}_n$, there are two types of β intervals: $\beta \in \tilde{A}_n = (\bar{\beta}_{n+1},\underline{\beta}_{n-1})$, where one symmetric solution of period $T = 2\pi(2n-1)/k$ is found and $\beta \in B_n = (\underline{\beta}_n,\bar{\beta}_{n+1})$, where two symmetric solutions of period $T = 2\pi(2n\pm1)/k$ exist. In [8] and [5] conditions for β were computed in order to have symmetric solutions of period $2\pi(2n-1)$ for the special cases $\alpha = 0$ and $\alpha = 2/3$ (k=1). If for $\alpha = 2/3$ we consider the range of β given by (4.2), we observe that this special case, studied in [5], is completely covered by the present results. Moreover, for $\alpha = 0$ the conditions on β match those of [8] for $\beta \to \infty$, see formulae (21) and (22) of [8]. In fig. 7 the functions p,q,I and T of α are plotted. Using this data we are in the position to construct regions Ω_n in the b,ν-plane, where the conditions for existence of a symmetric solution of period $T = 2\pi(2n-1)/k$ are satisfied. The following procedure has been carried out for k = 1, n = 1,2,3 and 4:
step 1. a value of ν is fixed, say $\nu = \nu^*$,
step 2. $\alpha = \alpha^*$ is determined such that $T(\alpha^*)\nu^* = 2\pi(n-\tfrac{1}{2})$,

step 3. the corresponding values of $\underline{\beta}_n$ and $\underline{\beta}_n$ are computed
step 4. the line $\nu = \nu^*$ is within Ω_n for $\alpha^* + \underline{\beta}_n/\nu^* < b < \alpha^* + \bar{\beta}_n/\nu^*$.
The result of this procedure, carried out for a sufficient number of values of ν, is depicted in fig. 8a. The boundaries of Ω_n for b small are computed from [8]. The shape of Ω_n agrees quite well with the results of FLAHERTY & HOPPENSTEADT [3], who integrated (1.1) numerically for a wide range of parameter and initial values, see fig. 8b.

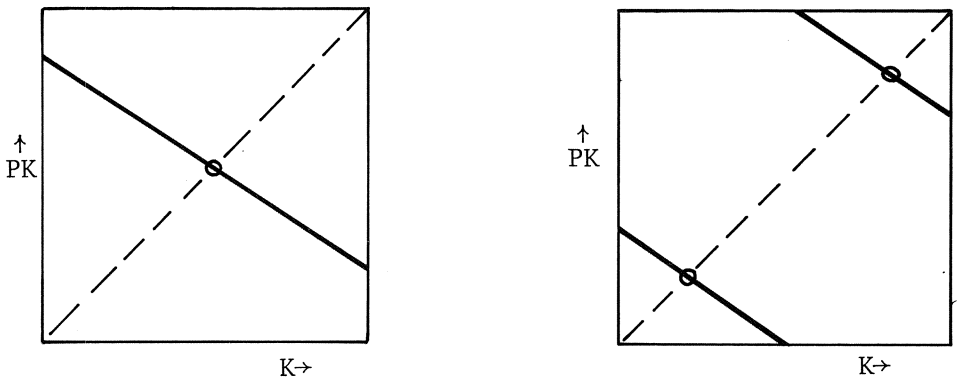

(a) case $\tilde{A}_n$ (b) case $\tilde{B}_n$

Fig. 6. Limit interval mapping, discontinuous at K = 0, mod(2πI).

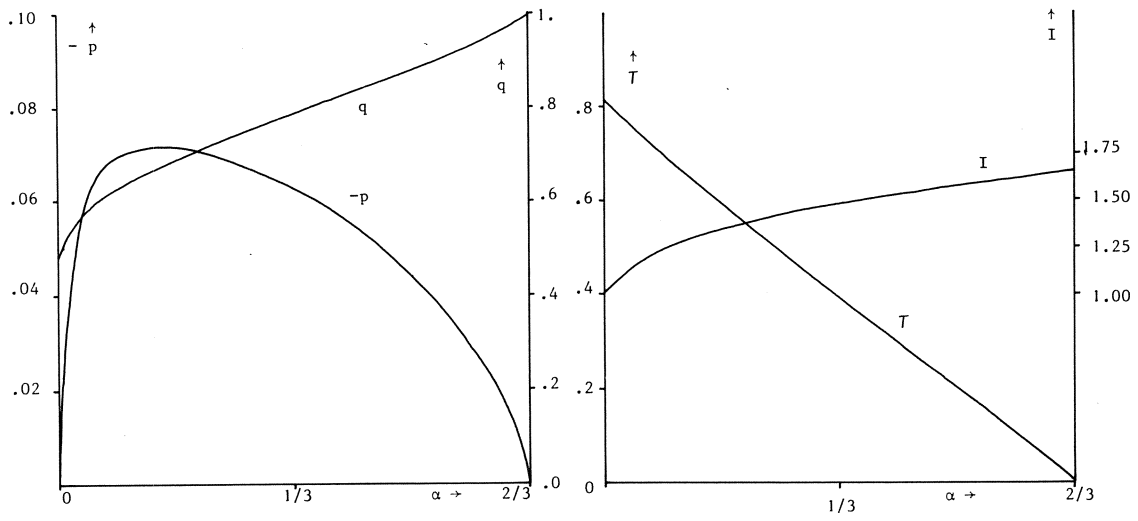

Fig. 7. the auxillary functions p,q I and T.

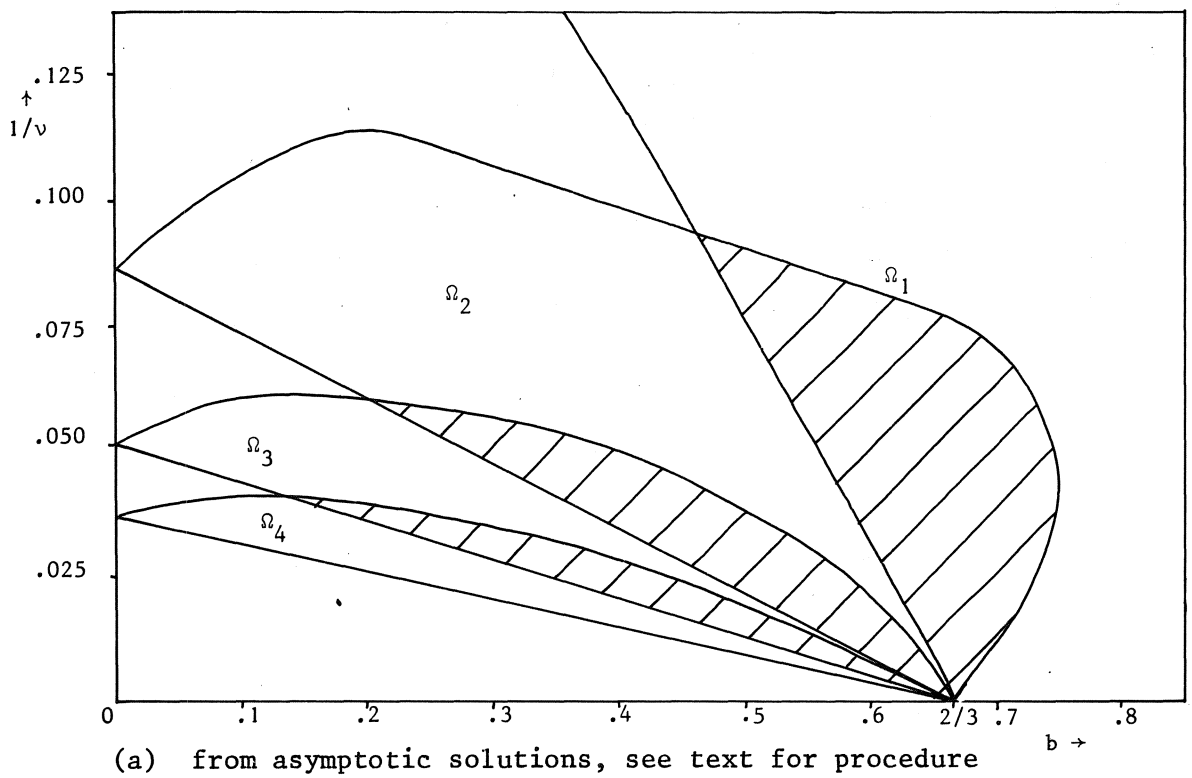

(a) from asymptotic solutions, see text for procedure

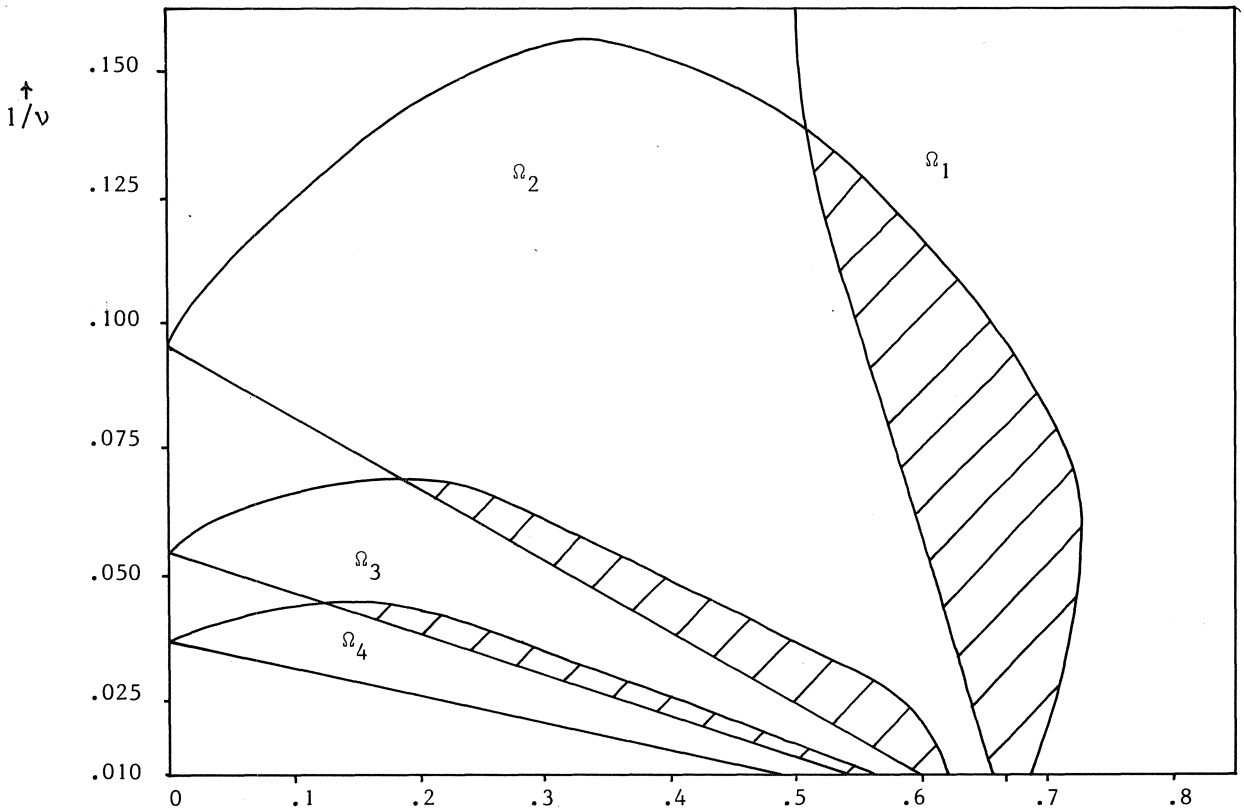

(b) from numerical solutions, after Flaherty and Hoppenstendt [3]

Fig. 8. The domains Ω_n with periodic solution $T = 2\pi(2n-1)$.

4.3. The case $\beta \in \tilde{A}_n$

In the discontinuous approximation we only found the stable fixed point; the unstable one is situated in the boundary layer, as is seen in fig. 9. Note that the X-interval has been shifted in order to have X = 0 in the interior of the interval. For any starting value different from the unstable fixed point the iterated solution will approach the stable fixed point.

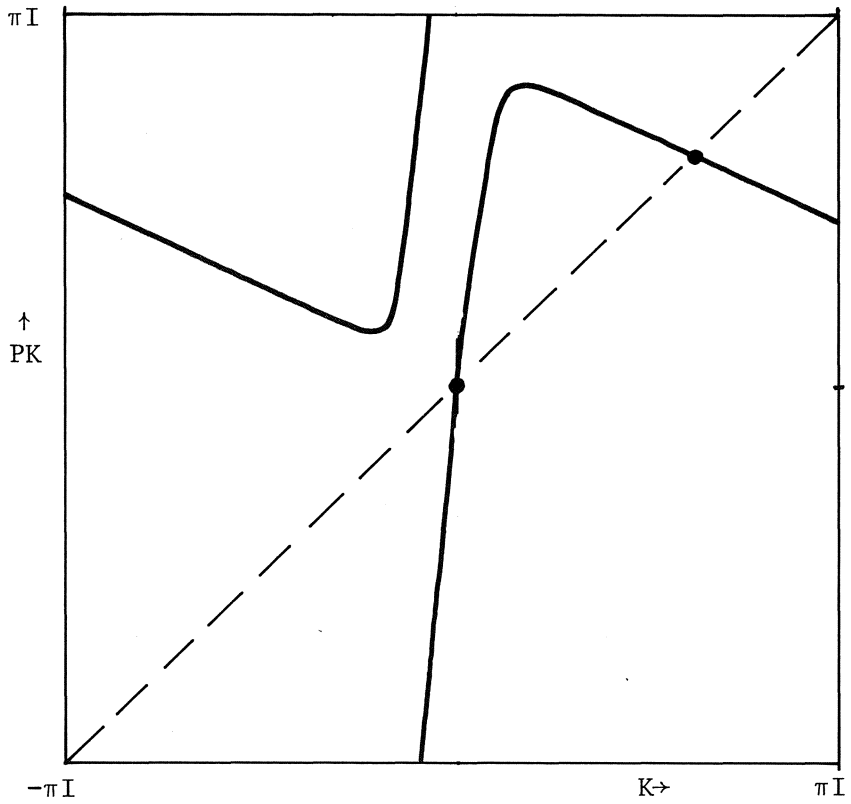

Fig. 9. The interval mapping for $\beta \in \tilde{A}_n$

4.4. The case $\beta \in \tilde{B}_n$

Besides the two stable fixed points of the discontinuous approximations, there are also two unstable ones within the boundary layer. The situation is now more complicated, as it is incorrect to assume that for any starting value, not coinciding with the unstable points, the iterated solution will tend to the two stable fixed points. There exists a non attracting subset of zero measure in which the iterated solution may go around in an irregular way. In order to describe this class of solutions we use symbolic dynamics, see section 2.2 and 2.3. As given in fig. 10 we consider subintervals V_i (i=0,1,2 and 3) and keep track of the mapping of points remaining in UV_i in the transition matrix

$$M = \begin{pmatrix} 0 & 1 & 1 & 1 \\ 0 & 1 & 1 & 1 \\ 1 & 0 & 0 & 0 \\ 0 & 1 & 1 & 1 \end{pmatrix} , \tag{4.3}$$

if $M_{ij} = 1$ a point V_i is mapped in V_j, while for $M_{ij} = 0$ such a mapping is not possible. As we described in section 2.3, the topological subspace Σ_M consisting of all biinfinite sequences of the symbols 0,1,2 and 3 is introduced allowing only combinations ij for which $M_{ij} = 1$, i.e. forbidden combinations in the set of sequences are 00,10,21,22,23 and 30. It is noted that the two unstable solutions are represented as sequences of just the symbol 1 and the symbol 3, respectively. Furthermore it is seen that the interval mapping discloses the dynamics of (1.1) to the same extent as the annulus mapping of section 2.2. The iterated solutions that correspond with an element of Σ_M have zero measure. Nevertheless they give us insight in the behavior of (1.1) with starting values chosen in such a way that the solution remains in UV_i a large (but finite) number of iterations of P before locking into a stable subharmonic. Initially such solutions behave in the irregular way as described here and the set of starting values has a measure different from zero.

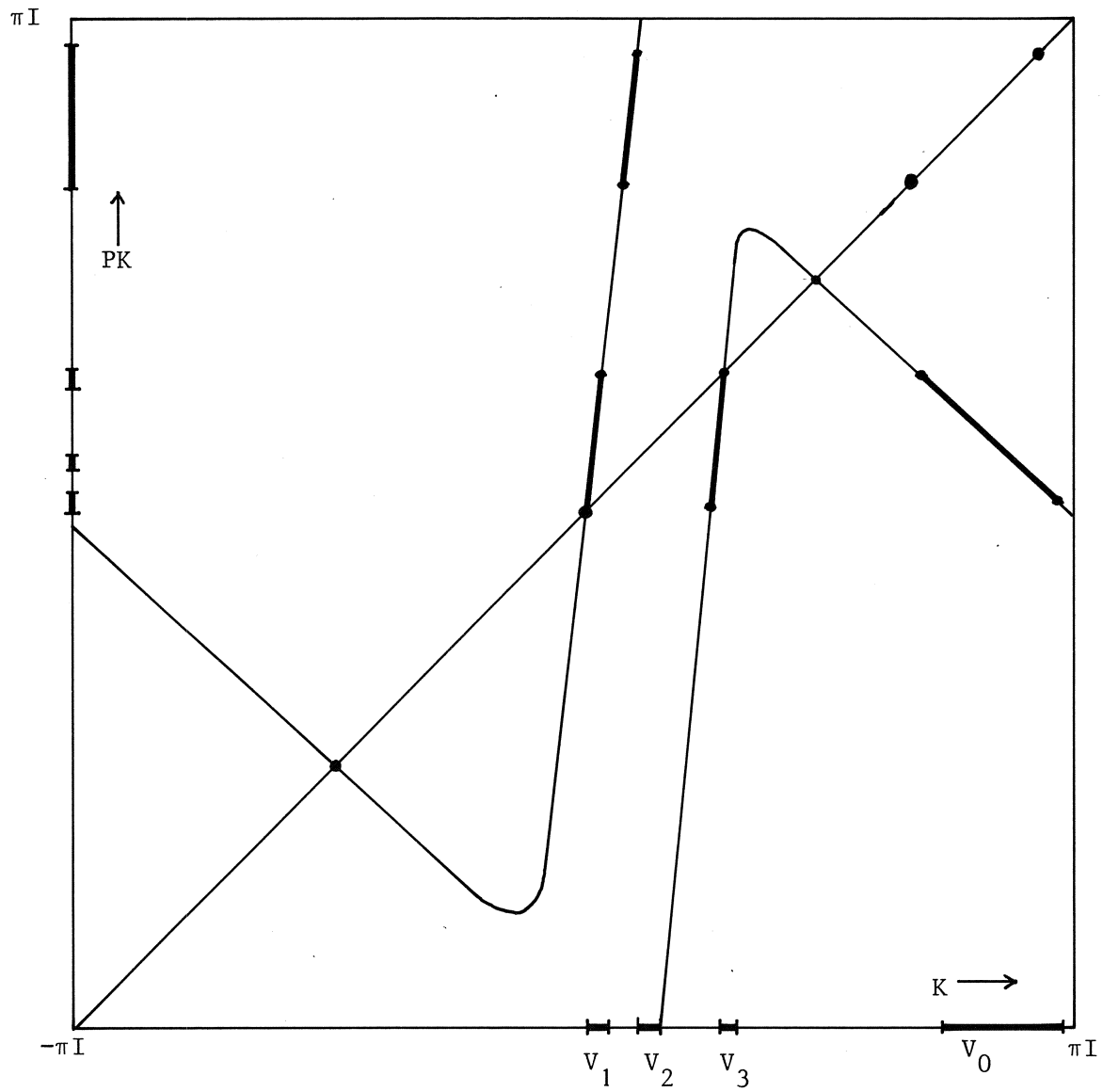

Fig. 10. The interval mapping for $\beta \in \tilde{B}_n$

4.5. The transitional case

In the discontinuous approximation of section 4.2 a third type of structure remained out of sight. We are aiming at the case of one stable fixed point with the point T below the unstable fixed point S, see fig. 11. Then

higher order stable fixed points of the iterated mapping are possible, as pointed out by LEVI [11]. His statement is based on a theorem of NEWHOUSE & PALIS [20]. In fig. 11 we sketch such a solution, while in the next section we will trace numerically one in a specific example.

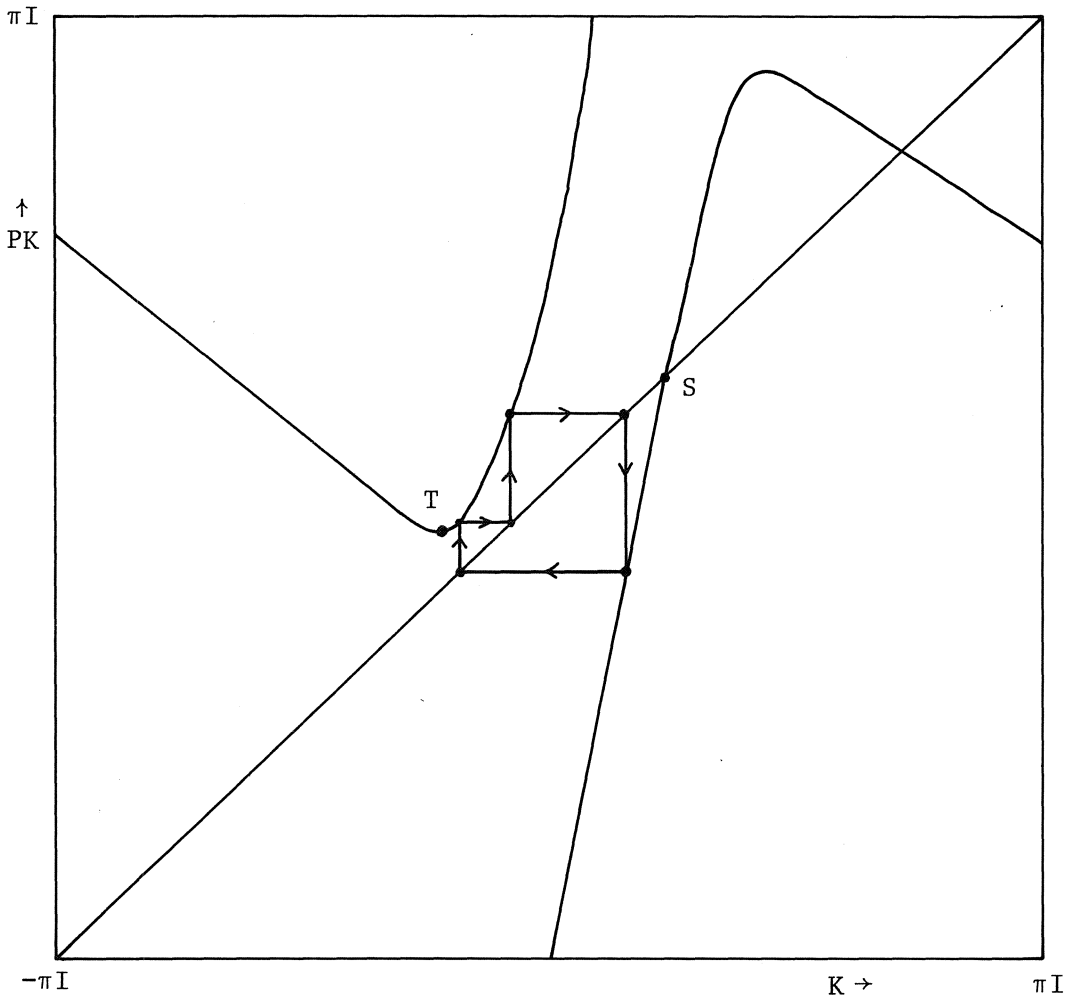

Fig. 11. The interval mapping for $\beta \in \tilde{g}_n$

4.6. A numerical approximation for $\alpha = 1/3$ and $\nu = 7.5$

Using analytical and numerical methods we found for $\alpha = 1/3$:

$$(4.4a)\qquad I = 3^{5/4}\{2E(\arcsin\sqrt{2/3(1-1/3\sqrt{3})},\ 1/3\sqrt{2-\sqrt{3}}) - F(\arcsin\sqrt{2/3(1-1/3\sqrt{3})},\ 1/2\sqrt{2-\sqrt{3}}) + 1/3(2-\sqrt{3})\sqrt{24+14\sqrt{3}}\}/\pi = 1.47597,$$

$$(4.4bcd)\qquad p = -0.061926,\ q = 0.788070,\ T = 0.392236,$$

where

$$(4.4e)\qquad E(\phi,k) = \int_0^{\phi} \sqrt{1-k^2\sin^2\theta}\ d\theta$$

$$(4.4f)\qquad F(\phi,k) = \int_0^{\phi} (\sqrt{1-k^2\sin^2\theta})^{-1}\ d\theta$$

In order to carry out the iterations of the mapping we approximate the mapping as follows. First a composite asymptotic solution is constructed. Since $dK/dt^* = 0$ in the endpoints $t^* = -\pi/2,\ 3\pi/2$, the boundary layer solution converges nonuniformly in these points as $dP/dK = dP/dt^*.\ dt^*/dK$. This is compensated by adding an asymptotically small correction to the composite asymptotic solution. For $K \in [0,\pi I]$ we have as a composite solution

$$(4.5a)\qquad K = \exp\{-d(t^*)\nu\}$$

$$(4.5b)\qquad d = \int_{t_{\frac{1}{2}}}^{t^*} \{\hat{x}^2(t;0)-1\}dt + 2\sin(t^*-\pi/2)\exp\{(t^*+\pi/2)(t^*-3\pi/2)\sqrt{\nu/2}/2)/\nu,$$

$$(4.5c)\qquad PK = C^+(t^*(K)) + R(n(K)) - qK,$$

while for $K \in [-\pi I,0]$

(4.5d) $\quad K = -\exp(-d(t^*))$

with t^* satisfying (4.5b) and

(4.5e) $\quad PK = C^-(t^*(K)) + R(n(K)) - qK.$

This composite expression is evaluated numerically in a set of points that have increasing density near K = 0: for n points we take

(4.6) $\quad K(j) = \pi I\exp\{-j\nu d(t_{3/2})/n\},$

then t^* follows from (4.5b). The value of PK is found from (4.5c) and (4.5e). In the computations a four point interpolation formula is used for the points (4.6), where PK is computed with a 6 decimal accuracy. Using this scheme we trace a stable fixed point of the second iterate by shifting the mapping in a vertical direction until in the iterated mapping two new fixed points arise, one of them being the stable fixed point we are looking for, see fig. 12 . It turns out that the stable solution has a very small domain of attraction and that it is only stable over an extremely small range of β. Therefore, we only give the value of the two new fixed points, which coincide within the accuracy we are working with. They arise at

$$K = -1.63402626$$

as β takes one of the values

$$\beta = 9.3770 - 5.3320(n-\tfrac{1}{2}), \quad n = 1,2,\ldots .$$

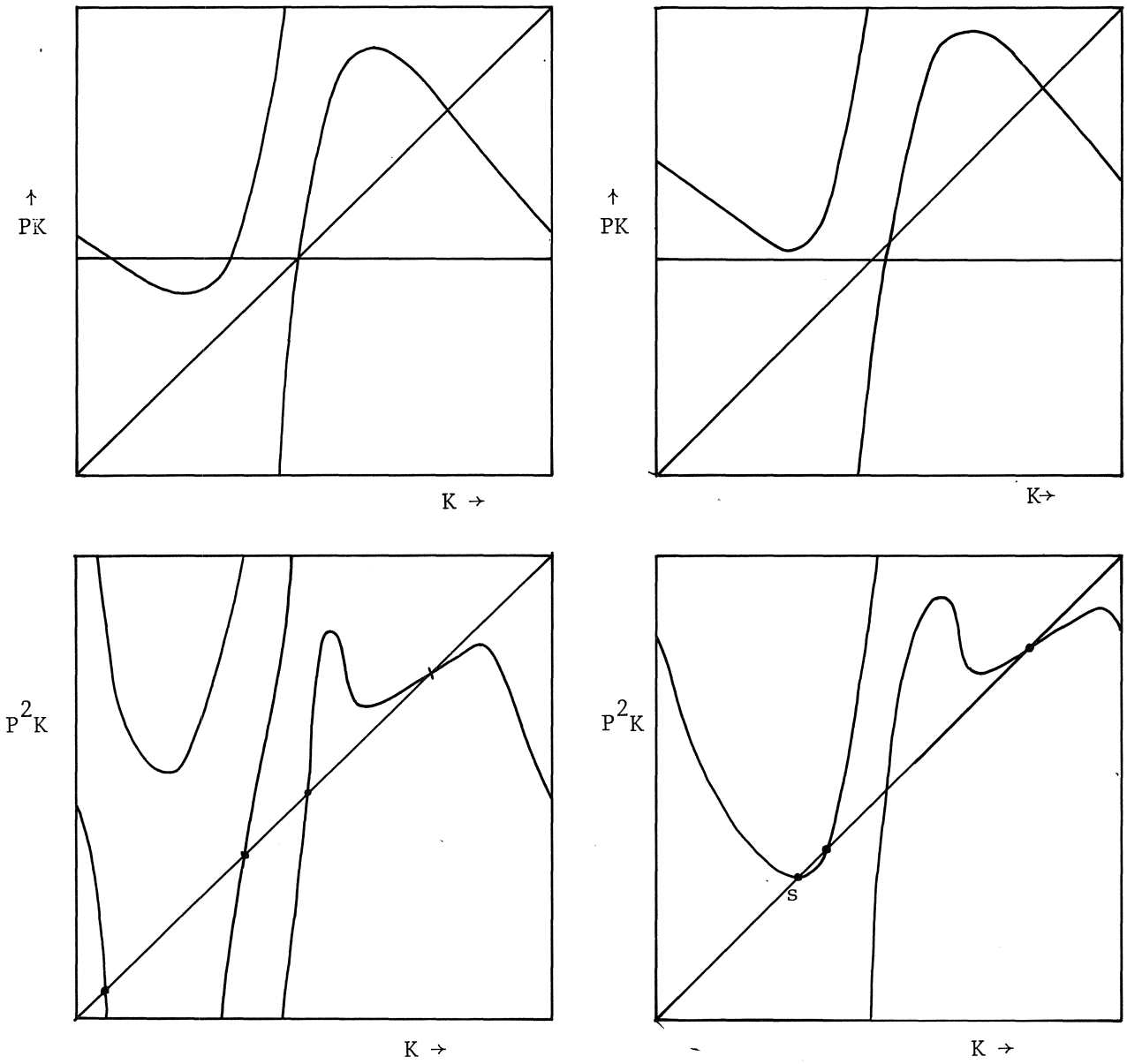

(a) all fixed points of P^2 not occurring for P are unstable for this value of β.

(b) one stable fixed point of P^2, not occurring for P, for this value of β.

Fig. 12. The occurence of irregular subharmonics

5. CONCLUDING REMARKS

As a result of our asymptotic analysis, we have obtained a completely determined relation between a continuous dynamical system and a mapping on a compact interval (a one-dimensional difference equation). This result is new in the sense that up to now, there has not been yet such a description of a continuous system having chaotic type of solutions in terms of a difference equation. For the Lorenz equations [17] with its strange attractor a comparison with a system of difference equations such as the Henon attractor is made, but the relation only refers to the occurence of a typical set of limit points in both cases. In the study of Levi a more specific qualitative relation between a continuous system and a difference equation was established. Levi expected the interval mapping to act upon a specific domain of the state space, see section 2.2. Likewise one describes the Lorenz equations by a mapping from a cross section of the state space into itself. From the present study we learn that there exists a typical difference variable which in this case turned out to be the index of a parabolic cylinder function, being part of a local asymptotic solution. It suggests that one has to look for characteristic quantities of a continuous system in order to relate it to a set of difference equations.

From the interval mapping the bifurcation pattern is understood for the various values of b. For the transitional domains $\tilde{g}_k$ the bifurcation structure turned out to be quite complex. It would be worthwhile to describe it in more detail using symbolic dynamics, as suggested in section 2.

Constructing a numerical approximation of the interval mapping as done in section 4.6, we touched upon two points needing some consideration. Firstly, the boundary layer solution appeared to be not differentiable in the end points, which was overcome by introduction of an asymptotically small correction term. Secondly, for $\nu = 7.5$ it was not possible to determine a stable irregular subharmonic for some β. From sharper calculations we concluded that even an accuracy of 14 decimals did not suffice. The reason for this is that the boundary layer in the interval mapping has a thickness of $O(\exp(-\nu))$. Consequently, the graph of P^2 has an extremely sharp peak at the point where it is about to be tangent to the diagonal, see fig. 12 . For stability it is necessary that $|dP^2/dK| < 1$ which is

only the case for β just past the point of tangency.

ACKNOWLEDGEMENT

The authors are grateful to J. Kok of the Department of Numerical Mathematics of the Mathematical Centre for his assistence in computing numerically the functions given in fig. 12 .

REFERENCES

[1] COLE, J.D., *Perturbation Methods in Applied Mathematics* (Blaisdell, Waltham, Mass., 1968).

[2] COLLET, P. & J.-P. ECKMANN, *Iterated Maps on the Interval as Dynamical Systems* (Birkhäuser, Basel, 1980).

[3] FLAHERTY, J.E. & F.C. HOPPENSTEADT, *Frequency Entrainment of a Forced Van der Pol Oscillator*, Stud. Appl. Math. 18 (1978) 5-15.

[4] GOLLUB, J.P., T.O. BRUNNER & B.G. DANLY, *Periodicity and Chaos in Coupled Nonlinear Oscillators*, Science 200 (1978) 48-50.

[5] GRASMAN, J., *Relaxation oscillations of a Van der Pol equation with large critical forcing term*, Quart. Appl. Math. 38 (1980) 9-16.

[6] GRASMAN, J., *On the Van der Pol relaxation oscillator with a sinusoidal forcing term*, Mathematisch Centrum Amsterdam, Report TW 207 (1980).

[7] GRASMAN, J., *Dips and slidings of the forced Van der Pol relaxation oscillator*, Mathematisch Centrum Amsterdam, Report TW 214 (1981).

[8] GRASMAN, J., E.J.M. VELING & G.M. WILLEMS, *Relaxation oscillations governed by a Van der Pol equation with periodic forcing term*, SIAM J. Appl. Math. 31 (1976) 667-676.

[9] GRASMAN, J., M.J.W. JANSEN & E.J.M. VELING, *Asymptotic methods for relaxation oscillations* in *Proceedings of the Third Scheveningen Conference on Differential Equations*, W. Eckhaus & E.M. de Jager,

eds., North-Holland Math. Studies 31 (North-Holland Publ. Comp., Amsterdam, New York, Oxford, 1978) pp. 93-111.

[10] GUCKENHEIMER, J., *Symbolic dynamics and relaxation oscillations*, Physica 1D (1980) 227-235.

[11] LEVI, M., *Qualitative analysis of the periodically forced relaxation oscillations*, Mem. Amer. Math. Soc. 244 (1981).

[12] LEVI, M., *Periodically forced relaxation oscillations in Global Theory of Dynamical Systems*, Z. Nitecki & C. Robinson, eds., Lecture Notes in Mathematics 819 (Springer-Verlag, Heidelberg, Berlin, Göttingen, 1980).

[13] LEVINSON, N., *A second order differential equation with singular solutions*, Ann. of Math. 50 (1949) 127-153.

[14] LI, T.-Y., & J.A. YORKE, *Period three implies chaos*, Amer. Math. Monthly 82 (1975) 985-992.

[15] LITTLEWOOD, J.E., *On Non-Linear Differential Equations of the Second Order*: III. *The Equation* $\ddot{y}-k(1-y^2)\dot{y}+y = b\mu k \cos(\mu t+\alpha)$ *for large* k, *and its Generalisations*, Acta Math. 97 (1957) 267-308.

[16] LITTLEWOOD, J.E., *On Van der Pol's equation with large* k in *Proceedings Symposium Nonlinear Problems*, R.E. Langer, ed. (University of Wisconsin Press, 1963) pp. 161-165, 174-175.

[17] LORENZ, E.N., *Deterministic nonperiodic flow*, J. Atmos. Sci. 20 (1963) 130-141.

[18] MAY, R.M., *Simple mathematical models with very complicated dynamics*, Nature 261 (1976) 459-467.

[19] MOSER, J., *Stable and Random Motions in Dynamical Systems*, Annals of Mathematics Studies 77 (Princeton University Press, Princeton, N.J., 1973).

[20] NEWHOUSE, S. & J. PALIS, *Cycles and bifurcation theory*, Astérisque 31 (1976) 43-140.

[21] RUELLE, D., *Strange Attractors*, Math. Intelligencer 2 (1980) 126-137.

[22] SHUB, M., *Stabilité globale des systèmes dynamiques*, Astérisque 56 (1978) 1-211.

[23] SMALE, S., *Diffeomorphisms with many periodic points* in *Differential and Combinatorial Topology*, S. Cairns, ed., Princeton Mathematical series 27 (Princeton University Press, Princeton, N.J., 1965) pp. 63-80.

[24] SMALE, S., *Differentiable dynamical systems*, Bull. Amer. Math. Soc. 73 (1967) 747-817.

[25] ŠTEFAN, P., *A Theorem of Šarkovski on the Existence of Periodic Orbits of Continuous Endomorphisms of the Real Line*, Comm. Math. Phys. 54 (1977) 237-248.